

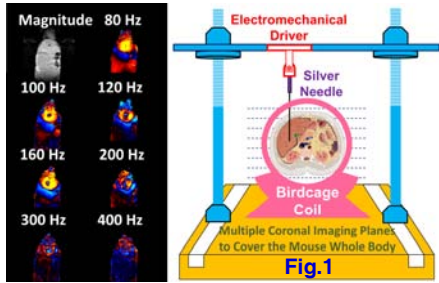
Advanced Assessment of Liver Diseases with Magnetic Resonance Elastography in Mouse Models

Meng Yin¹, Douglas A. Simonetto², Jason L. Bakeberg³, Anuradha Krishnan², Kevin J. Glaser¹, Vijay H. Shah², Christopher J. Ward³, Peter C. Harris³, Michael R.

Charlton², Armando Manduca¹, and Richard L. Ehman¹

¹Radiology, Mayo Clinic, Rochester, Minnesota, United States, ²Gastroenterology and Hepatology, Mayo Clinic, Rochester, Minnesota, United States, ³Nephrology and Hypertension, Mayo Clinic, Rochester, Minnesota, United States

Introduction: To reduce biopsy-related complications and sampling errors, hepatic MR Elastography (MRE) has been developed as a safe, more comfortable, and less expensive noninvasive alternative to liver biopsy for diagnosing hepatic fibrosis (1-3). Recently, many studies have shown that the mechanical properties of liver tissue appear promising for the differentiation of several pathologic conditions of the liver (4-7). For instance, liver stiffness can have a static component that is mainly determined by extracellular matrix composites and structure (e.g., hepatic fibrosis), and a dynamic component that is affected by intrahepatic hemodynamic changes (e.g., inflammation and portal hypertension) (8,9). It is likely that independent mechanical properties other than "shear stiffness", including other model-free properties (e.g., the complex shear modulus, shear wave attenuation and the frequency dispersion of mechanical properties) or model-based viscoelastic parameters, will improve the identification of specific pathophysiologic changes of the liver. Before liver MRE is adopted as a primary tool for monitoring liver disease progress, we need a comprehensive assessment of which hepatic tissue mechanical properties are sensitive to specific microstructure constitutions and pathophysiological states.



Methods and Materials: All experiments were implemented on a 3.0-T whole-body GE imager (HDx, GE Healthcare, Milwaukee, WI), using a custom birdcage coil. Fig. 1 (right) demonstrates our experimental setup. A silver needle is used to generate shear waves throughout the liver. The mice were anesthetized with 1.0-1.5% isoflurane. As shown in Fig.1 (left), wave images were acquired with a multislice, spin-echo EPI MRE sequence with three motion-encoding directions using seven different harmonic vibrations at frequencies of 80, 100, 120, 160, 200, 300, 400 Hz. The acquired 3-D/3-axis wave data had a resolution of $0.3 \times 0.3 \times 2 \text{ mm}^3$. They were interpolated to $0.15 \times 0.15 \times 2 \text{ mm}^3$ and filtered with the curl operator to remove undesired bulk motion, processed with 20 evenly spaced 3-D directional filters (radial bandpass filter: 4th-order Butterworth filter, cut-off frequencies = (0.001, 24) cycles/FOV), smoothed with a $3 \times 3 \times 3$ quartic kernel and then inverted with a direct inversion of the Helmholtz equation to calculate the complex shear modulus. Nine well-established viscoelastic models (10-13) were applied to calculate mechanical properties of the liver. All quantities were reported as means and standard deviations of ROIs drawn to encompass as much of the liver as possible that had significant wave propagation. Statistical analysis was performed with a two-sided paired t-test and 5% significance.

Three mouse models were used: Exp.1) Knockout PKD (polycystic kidney disease) mouse model with early onset of hepatic inflammation: 36 age- and gender-matched PKD and control mice 1, 3 and 6 months old; Exp.2) NASH (nonalcoholic steatohepatitis) mouse model with steatosis, inflammation and fibrosis: 12 age-matched male mice with 9 months feeding on a fast food diet (FFD: 7) or standard chow (SC: 5); Exp.3) pIVCL (partially inferior vena cava ligation) mouse model with hepatic congestion: 8 pIVCL mice and 5 age-matched SHAM mice at 2, 4, and 6 weeks post-surgery. Portal pressure was obtained in all pIVCL and SHAM mice immediately after the MR exam.

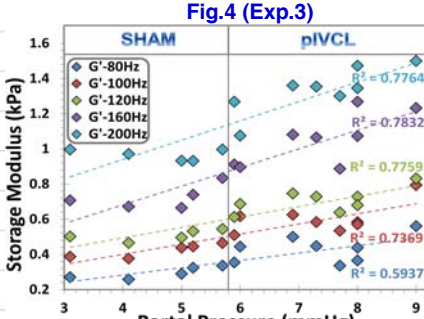
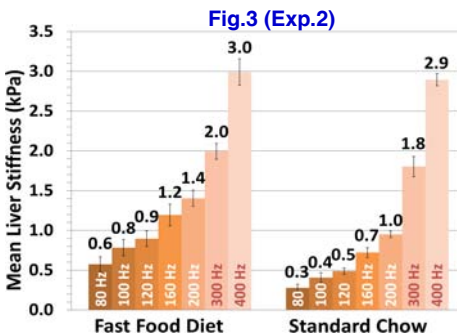
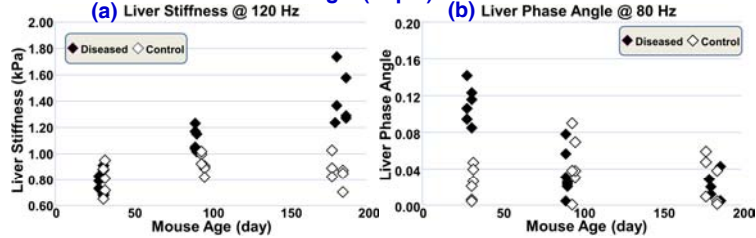


Fig.2 (Exp.1)



Results: Knockout PKD mice carry chronic fibrotic and cystic liver disease from birth. They usually have histologically observable hepatic inflammation right after weaning (1 month old), then develop progressive hepatic fibrosis when they get older (3 and 6 months old). Compared with the control groups, liver stiffness was significantly elevated in 3- and 6-month-old PKD mice, but had no significant change in 1-month-old PKD mice (Fig.2a). In contrast, phase angle cannot detect fibrosis in older mice, but it can distinguish early onset of inflammation in 1-month-old mice (Fig.2b).

NASH mice had significantly higher liver stiffness and stiffness frequency dispersion than the control group within the frequency range of 80 to 200 Hz (Fig.3). Significant differences were also found in many properties derived from various viscoelastic models as shown in Table 1. In pIVCL and SHAM mice, significant correlations were observed between portal pressure and storage modulus (Fig.4), and many derived viscoelastic properties as shown in Table 2. However, no significant correlations were found with the loss modulus, phase angle and viscosity parameters.

Discussion and Conclusion: Results in Exp.1&2 demonstrate that the phase angle of the complex shear modulus (Fig.2) can be used to discriminate between inflammation alone and fibrosis in early-stage disease, while stiffness or other parameters (Table 1) may be better discriminators in later stages. From a clinical perspective, this differentiation is more important in early stages of disease. Liver congestion, an important confounding factor in liver stiffness elevation, is common in patients with congenital heart disease, right-sided heart failure or Budd-Chiari syndrome. The results in Exp.3 (Table 2) suggest that some of these parameters, particularly the Jeffreys and Fractional Derivative models, have promise for predicting the degree of liver congestion, which currently can only be assessed with invasive portal pressure measurement.

References: 1. Yin M, CGH 2007; 2. Asbach P, MRM 2008; 3. Huwart L, Gastroenterology 2008; 4. Yin M, TMRI 2009; 5. Barry CT, UMB 2012; 6. Tapper EB, CGH 2012; 7. Ding H, JHUST 2012; 8. Yin M, ISMRM 2009, 110; 9. Yin M, ISMRM 2010, 256; 10. Klatt D, Phys Med Biol 2007; 11. Sack I, Neuroimage 2009; 12. Suki B, J Appl Physiol 1994; 13. Robert B, IEEE 2006.